



Faculty of Electrical Engineering

**MINIMIZATION OF TORQUE RIPPLE AND FLUX DROOP USING
OPTIMAL DTC SWITCHING AND SECTOR ROTATION
STRATEGY**

اونيورسي تيكنيكل مليسيا ملاك
UNIVERSITI TEKNIKAL MALAYSIA MELAKA

Siti Azura Binti Ahmad Tarusan

Doctor of Philosophy

2022

**MINIMIZATION OF TORQUE RIPPLE AND FLUX DROOP USING OPTIMAL
DTC SWITCHING AND SECTOR ROTATION STRATEGY**

SITI AZURA BINTI AHMAD TARUSAN

**A thesis submitted
in fulfilment of the requirements for the degree of Doctor of Philosophy**



UNIVERSITI TEKNIKAL MALAYSIA MELAKA

2022

DECLARATION

I declare that this thesis entitled “Minimization of Torque Ripple and Flux Droop using Optimal DTC Switching and Sector Rotation Strategy” is the result of my own research except as cited in the references. The thesis has not been accepted for any degree and is not concurrently submitted in candidature of any other degree.



Signature

:

Name

:

Siti Azura Binti Ahmad Tarusan

Date



:

06/09/2022

UNIVERSITI TEKNIKAL MALAYSIA MELAKA


APPROVAL

I hereby declare that I have read this thesis and in my opinion this thesis is sufficient in terms of scope and quality for the award of Doctor of Philosophy.

 Signature : 

Supervisor Name : Associate Professor Dr. Mohd Luqman Mohd
Jamil

Date : 06/09/2022



اونيورسيتي تيكنيكل مليسيا ملاك
UNIVERSITI TEKNIKAL MALAYSIA MELAKA

DEDICATION

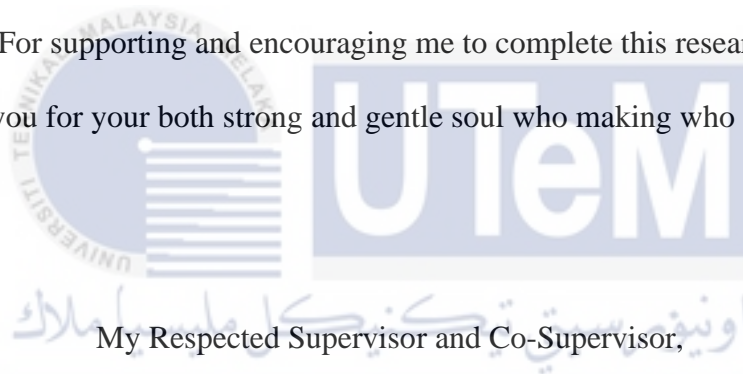
Special Dedication to:

My Beloved Parents,

Ahmad Tarusan Bin Abu and Ros Binti Othman

For supporting and encouraging me to complete this research

Thank you for your both strong and gentle soul who making who I am today



My Respected Supervisor and Co-Supervisor,

Assoc. Prof. Dr. Mohd Luqman Bin Mohd Jamil and Dr Auzani Bin Jidin

Thank you for your both strong support, motivation, guidance and supervision to
accomplish this research

May God bless and protect them with happiness

ABSTRACT

Direct Torque Control (DTC) is a well-known AC control scheme for its robustness and simplicity. Although DTC provides excellent dynamic torque control performance, but it has several drawbacks. The digital implementation of the hysteresis band controller, which causes a delay action, may result in huge ripple and switching frequency inconsistency for DTC torque performance. Since the torque slope is already disturbed in the hysteresis bandwidth in various operating conditions, the limiting voltage vector of the two-level inverter in the conventional DTC limits the control switching frequency in the hysteresis controller. Another drawback of conventional DTC is that the presence of voltage drop in a stator resistance at low operating speeds causes a droop in stator flux performance. This problem occurs as the voltage vectors deviate from the usual state, where it manifests itself as a change in the boundary sector of the circular flux locus. Therefore, an optimal DTC switching strategy and an optimal DTC sector rotation strategy to overcome the problems in a three-phase induction motor have been proposed. A five-level cascaded H-bridge (CHB) inverter was used in the optimal DTC switching strategy because it had many voltage vectors and could be used for a variety of speed operations. Its objectives were to propose the optimal switching vector in minimizing torque ripple and controlling switching frequency at the steady-state of various speed operations. A modification torque error status and a look-up table of a five-level CHB inverter were used to implement the specified optimal voltage vectors. Another objective was to formulate and evaluate the optimal DTC sector rotation strategy that can reduce stator flux droop in the variation of torque and speed in steady-state and dynamic response. The optimal sector rotation strategy is determined using an analytical model of shifted angle that incorporates speed and torque variables which is dynamically tuned. Both proposed strategies were compared with conventional method and verified through simulation and experimentation works. MATLAB/Simulink software is used to simulate the proposed strategies while a complete setup system consists of a DS1104 digital signal processor (DSP)-board (to implement the DTC algorithm), Field-programmable Gate Arrays (FPGA) (to implement the blanking circuit), two-level and five-level (CHB) inverter circuit, gate driver circuit, and a 1.1 kW induction motor with 2 kW DC generator as a load is developed for testing and verification purpose. A compromise between simulation and experimentation works resulted in significant improvements; 1) a reduction of torque ripple up to 50% and a reduction of switching frequency up to 40%, 2) an ability to maintain a similar magnitude of stator flux by eliminating the droops. In conclusion, the method introduced demonstrates the effectiveness of DTC performance which maintains its simple structure as well as offers ease in modification for a desired control purpose.

PENGURANGAN RIAK DAYAKILAS DAN KEJATUHAN FLUKS MENGGUNAKAN STRATEGI PENSUISAN DTC DAN PUTARAN SEKTOR YANG OPTIMUM

ABSTRAK

Kawalan Dayakilas Langsung (DTC) diakui sebagai satu keteguhan dan struktur kawalan AC yang ringkas. Walaupun DTC menyediakan prestasi cemerlang kawalan dayakilas yang dinamik, tetapi ia menyebabkan beberapa kekurangan. Pelaksanaan digital pengawal jalur histerisis, yang memicu tindakan lengah, boleh mengakibatkan riak besar dan ketidakseragaman pensuisan frekuensi untuk prestasi dayakilas DTC. Oleh kerana kecerunan dayakilas terganggu dalam lebar jalur histerisis dalam pelbagai keadaan operasi, vektor voltan penyongsang dua peringkat yang terhad dalam DTC konvensional telah menghadkan frekuensi pensuisan kawalan dalam pengawal histeresis. Satu lagi kelemahan DTC konvensional ialah penurunan voltan dalam rintangan pemegun pada operasi kelajuan rendah yang menyebabkan penurunan prestasi fluks pemegun. Masalah ini berlaku apabila vektor voltan menyimpang daripada keadaan biasa, di mana ia dipamerkan sebagai satu perubahan dalam sempadan sektor lokus fluks bulatan. Oleh itu, strategi pensuisan DTC dan strategi putaran sektor DTC yang optimum untuk mengatasi masalah dalam motor aruhan tiga fasa telah dicadangkan. Penyongsang tetimbang-H lima-peringkat (CHB) telah digunakan dalam strategi pensuisan optima DTC kerana ia mempunyai banyak vektor voltan dan boleh digunakan untuk pelbagai operasi kelajuan. Objektifnya adalah untuk mencadangkan pensuisan vector yang optimum dalam meminimumkan dayakilas riak dan mengatur frekuensi pensuisan pada keadaan mantap pelbagai operasi kelajuan. Pengubahsuaian status ralat dayakilas dan jadual carian bagi penyongsang CHB lima-peringkat telah digunakan bagi melaksanakan penentuan vektor voltan yang optima. Satu lagi objektif adalah untuk merumus dan menilai putaran sektor DTC yang optimum yang boleh mengurangkan kejatuhan fluks pemegun dalam variasi dayakilas dan kelajuan dalam keadaan mantap dan tindak balas dinamik. Strategi putaran sektor optimum ditentukan menggunakan model analitik peralihan sudut yang menggabungkan pembolehubah kelajuan dan dayakilas yang ditala secara dinamik. Kedua-dua strategi yang dicadangkan telah dibandingkan dengan kaedah konvensional dan disahkan melalui kerja-kerja simulasi dan eksperimen. Perisian MATLAB/Simulink digunakan untuk mensimulasikan strategi-strategi yang dicadangkan manakala sebuah sistem binaan lengkap terdiri daripada papan pemproses isyarat digital (DSP) DS1104 (untuk melaksanakan algoritma DTC), Tatasusunan Gerbang Medan Terprogram (FPGA) (untuk melaksanakan litar padaman), litar penyongsang dua-aras dan lima-aras (CHB), litar pemacu get, dan motor aruhan 1.1 kW dengan penjana DC 2 kW sebagai beban dibangunkan untuk tujuan ujian dan pengesahan. Kompromi antara kerja-kerja simulasi dan eksperimen menghasilkan penambahbaikan yang ketara; 1) pengurangan riak dayakilas sehingga 50% dan pengurangan frekuensi pensuisan sehingga 40%, 2) keupayaan menyingkirkan kejatuhan untuk mengekalkan magnitud fluks pemegun yang serupa. Kesimpulannya, kaedah yang diperkenalkan menunjukkan keberkesanan prestasi DTC yang tetap mengekalkan struktur ringkasnya serta menawarkan kemudahan dalam pengubahsuaian untuk sesuatu tujuan kawalan yang dikehendaki.

ACKNOWLEDGMENTS

In the name of Allah, the Most Gracious and the Most Merciful. Alhamdulillah, I praise and thank Allah SWT for His greatness and for giving me the strength and courage to complete this thesis entitled An Optimal DTC Switching and Sector Strategies for A Three Phase Induction Motor.

First and foremost, I would like to express my deepest gratitude and appreciation to Universiti Teknikal Malaysia Melaka (UTeM) that gives me opportunity in gaining knowledge and soft skills. Then, the special thanks were given to Assoc. Prof. Dr. Mohd Luqman Bin Mohd Jamil and Dr. Auzani Bin Jidin for their valuable guidance and knowledge. The support supervision under them in the positive environment was truly help for smoothness of my PhD progress. Although I had lack in many ways and sometimes been in the grief situation and condition, but they continued to never give up on me and always increased up the desired mood of my study.

At the same time, I would like to express my gratitude to many people who contributed to this research. I would like to thank to ex-master student, Mr. Muhd Khairi for spending him time to teach and guide me deeply about this project in the short time period. Subsequently, to other my colleagues in the same department such as Assoc. Prof. Dr. Raja and Assoc. Prof. Dr. Kasrul who shared some opinions and knowledges in order to accomplish this project. Then, to the other member of research lab (PED and EMD) and the rest who became my physically and emotionally support as well as closed to me during this work alone project. Thousands of appreciations and thanks to anyone whom involved either directly or indirectly helped me in this project.

Finally, privileges of appreciation and affection were directly to my parents and siblings for their support and encouraging me to never give up in completing this PhD thesis.

TABLE OF CONTENTS

DECLARATION	i
APPROVAL	ii
DEDICATION	iii
ABSTRACT	iv
ABSTRAK	vii
ACKNOWLEDGMENTS	viii
TABLE OF CONTENTS	xxi
LIST OF TABLES	xxii
LIST OF FIGURES	xxiv
LIST OF APPENDICES	xxviii
LIST OF ABBREVIATION	
LIST OF SYMBOLS	
LIST OF PUBLICATIONS	
CHAPTER 1	1
1. INTRODUCTION	1
1.1 Research background	1
1.2 Problem statement	6
1.3 Research objectives	10
1.4 Research scope	10
1.5 Research limitation	11
1.6 Research flow outlines	12
1.7 Thesis outlines	14
CHAPTER 2	16
2. LITERATURE REVIEW	16
2.1 Induction machine in AC drives	16
2.2 The configuration of DTC	20
2.2.1 The conventional inverter	21
2.2.1.1 The basic structure of conventional inverter	21
2.2.1.2 The relationship between VSI with three-phase machine	23
2.2.2 The principle of DTC	26
2.2.2.1 Direct flux control	26
2.2.2.2 Direct torque control	29
2.2.3 Look-up table of DTC	33
2.2.4 Estimation model	34
2.3 The limitation of hysteresis-based DTC	37
2.4 Development of stator flux droop in DTC	42
2.5 Several improvements of DTC	43
2.5.1 Modified look-up table	43
2.5.2 Improved hysteresis comparators	49
2.5.3 Carrier frequency switching	51

2.5.4	Voltage balancing strategy	53
2.5.5	Duty cycle-based strategy	54
2.5.6	Virtual vector	56
2.5.7	Sensorless control	58
2.5.8	Intelligent/linearization control	60
2.5.9	DTC using space vector pulse width modulation (SVPWM)	62
2.5.9.1	The principal of SVPWM	64
2.5.9.2	DTC-SVM in MLI	68
2.6	Literature finding and research gap	70
2.7	Conclusion	72

CHAPTER 3		73
3. RESEARCH METHODOLOGY		73
3.1	Research implementation flowchart	74
3.2	Mathematical model of induction motor	76
3.3	Multilevel inverter (MLI)	81
3.3.1	Five-level cascaded H-bridge inverter	81
3.3.2	Identification of flux sectors	83
3.3.3	Look-up table for five-level CHB (DTC)	86
3.4	Investigation of the DTC characteristic	88
3.4.1	Load angle in the principal of torque control	88
3.4.2	The effect of different voltage vector applications on torque behaviour	91
3.4.3	The comparison of low-speed and high-speed operation in DTC	94
3.5	DTC development by using optimal DTC switching strategy	96
3.5.1	Improvement 1: Minimization of control switching frequency	96
3.5.2	Improvement 2: Reduction of torque ripple	105
3.5.3	Optimal voltage vector based on the torque error status	112
3.5.4	Proposed DTC structure of optimal switching strategy	116
3.6	Investigation of stator flux droop performance	117
3.7	DTC development by using optimal sector rotation strategy	122
3.7.1	Proposed DTC structure of optimal sector rotation strategy	125
3.8	Simulation Setup	126
3.8.1	The simulation diagram of the conventional and proposed DTC	126
3.8.2	Flux controller	129
3.8.3	Torque controller	129
3.8.4	Three-phase induction motor	130
3.8.5	Stator voltage component	131
3.8.6	Electromagnetic torque and stator flux estimation	132
3.8.7	Proposed block	132
3.8.8	Detection of flux sector	134
3.8.9	Look-up table for selecting voltage vector	135
3.9	Experimental setup	136
3.9.1	DS1104 R&D controller board	137
3.9.2	Current measurement circuit	140
3.9.3	Field programmer gate array (FGPA) / DEO Nano board	141
3.9.4	Power circuit or voltage source inverter and gate drives	144
3.9.5	Induction motor	147
3.10	Conclusion	149

CHAPTER 4	151
4. RESULT AND DISCUSSION	151
4.1 Control switching frequency performance analysis in DTC five-level CHB	151
4.2 Control switching frequency and torque ripple reduction at constant torque control	161
4.3 Stator flux droop performance in the conventional DTC	172
4.3.1 Analysis of stator flux effect based on the speed variation using fixed sector rotation strategy	173
4.3.2 Analysis of stator flux effect based on the speed and torque variation using fixed sector rotation strategy	176
4.3.3 Stator flux droop improvement using optimal sector rotation strategy	182
4.4 Conclusion	191
 CHAPTER 5	 192
5. CONCLUSION AND FUTURE WORK	192
5.1 Conclusions	192
5.2 Research contributions	193
5.3 Suggestions for future work	194
 REFERENCES	 195
APPENDICES	214



LIST OF TABLES

TABLE	TITLE	PAGE
2.1	The lookup table of conventional DTC (Takahashi and Noguchi, 1986)	34
3.1	The look-up table for five-level CHB	87
3.2	The suitable amplitude of vector selection in the conventional DTC	113
3.3	The suitable amplitude of vector selection in the proposed method	115
3.4	MATLAB/Simulink simulation parameter	128
3.5	Parameter of induction motor and DC generator	149
4.1	The evaluation of DTC performance for each classification of operating speed	172
4.2	The result of the stator flux droop at various operating speed	176
4.3	The result of the stator flux droop at various operating speed and torque	181
4.4	The summary result using optimal sector rotation strategy	190

LIST OF FIGURES

FIGURE	TITLE	PAGE
1.1	The configuration of FOC scheme (Reza et al., 2014)	2
1.2	The configuration of DTC scheme (Takahashi and Noguchi, 1986)	3
1.3	The large torque ripple problem in DTC through; the torque and torque error status waveform (left) and the selected vector on mapping vector (right) as highlighted by Takahashi and Noguchi (1986)	6
1.4	The limitation of stator flux in conventional DTC shown through; the circular locus flux (left) and the simulation waveform (right) as highlighted by Takahashi and Noguchi (1986)	8
2.1	Direct method of field-oriented control (Sen, 1990)	18
2.2	Indirect method of field-oriented control (Sen, 1990)	18
2.3	The configuration of conventional DTC (Takahashi and Noguchi, 1986)	20
2.4	Two-level inverter circuit (Abu-Rub et al., 2012)	21
2.5	The d-q plane mapping of three phase quantities (Abu-Rub et al., 2012)	23
2.6	Mapping voltage vector two-level inverter circuit (Kumar et al., 2018)	25
2.7	(a) Six sectors in division of stator flux plane and (b) Two particular active voltage vectors control the stator flux within its hysteresis band on sector I and II (Rahim, 2016)	27
2.8	(a) Two-level hysteresis comparator and (b) The waveform diagram	28

	of stator flux (Rahim, 2016)	
2.9	The variation of δ_{sr} with application the probability voltage vector (Idris, 2000)	30
2.10	DTC induction machine drive in four-quadrant operation (Idris, 2000)	31
2.11	(a) Three-level hysteresis comparator and (b) The waveform diagram of torque (Rahim, 2016)	32
2.12	The estimation of voltage model (Bose Bimal K., 2002)	36
2.13	The estimation of current model (Bose Bimal K., 2002)	37
2.14	The condition of variable control switching frequency and large torque ripple through; (a) the reference and estimated torque, (b) the torque error and (c) torque error status observed in the conventional DTC by Takahashi and Noguchi (1986)	38
2.15	The switches of voltage vector at the boundary of sector in the conventional DTC by Takahashi and Noguchi (1986)	39
2.16	The waveform condition of the sector boundary in the conventional DTC by Takahashi and Noguchi (1986)	39
2.17	Three-level inverter or classic MLI (a) Flying Capacitor (FC), (b) Neutral Point Clamped (NPC) and (c) Cascaded H-Bridge (CHB) (Abd Halim et al., 2016)	45
2.18	Mapping voltage vector of (a) three-level (Usta et al., 2017) and (b) five-level (Nordin et al., 2016)	45
2.19	Hybrid multilevel inverter using dual DC sources feeding open-end-winding (Venugopalan, 2019)	46
2.20	Matrix converter schematic configuration (Casadei et al., 2001)	47
2.21	The structure of (a) output line-to-neutral voltage vector and (b) input	47

	line current vector (Benachour et al., 2017)	
2.22	(a) Two-level inverter and (b) mapping voltage vector for five-phase machine (Parsa and Toliyat, 2007)	48
2.23	Hysteresis comparator of (a) 7-level for torque and (b) 2-level for flux (Nair et al., 2013)	51
2.24	Hysteresis comparator of (a) 7-level for torque and (b) 5-level for flux (Nair et al., 2013)	51
2.25	Carrier frequency controller in conventional DTC (N.R.N. Idris and Yatim, 2002)	52
2.26	Proposed frequency controller in MLI (Nordin et al., 2016)	53
2.27	Voltage balancing strategy in NPC-DTC (Ismail et al., 2015)	54
2.28	Duty cycle based strategy in conventional DTC (Kang and Sul, 1999)	56
2.29	Duty cycle based strategy in DTC using MLI applying (a) conventional method (contain LVV/MVV, SVV and ZVV) and (b) proposed method (contain LVV/MVV and VVV) (Mohan et al., 2017)	56
2.30	Mapping vector of five-phase machine in (a) $\alpha\beta$ plane and (b) xy plane (Payami and Behera, 2017)	58
2.31	Virtual vector of five-phase machine (Payami and Behera, 2017)	58
2.32	(a) Block diagram of sensorless and (b) Structure of speed adaptive flux observer (Usta et al., 2015)	60
2.33	(a) Fuzzy logic controller for CHB-DTC represented by block diagram and (b) Membership function of fuzzy logic controller (Mortezaei et al., 2011)	62
2.34	The configuration of DTC by using SVPWM strategy (Lascu et al., 2000)	63
2.35	Space vector of two-level inverter with a reference vector, \vec{v}_S^*	65

	(Lascu et al., 2000)	
2.36	The reference voltage in SVPWM strategy as referred in (2.36) (Lascu et al., 2000)	67
2.37	Torque variation influenced by the generation and effect of switching vectors (Rahim, 2016)	67
2.38	The comparison location of reference voltage in SVPWM between (a) two -level and (b) three-level inverter (Gupta and Khambadkone, 2007)	68
2.39	The comparison of torque variation influenced by the generation and effect of switching vectors between two-level inverter and three-level inverter (Rahim, 2016)	70
2.40	A diagram review of DTC via implemented of MLI	71
3.1	The flowchart of research implementation	76
3.2	The structural view of the symmetrical two-pole machine (Bose Bimal K., 2002)	78
3.3	The configuration of; a) single-phase and b) three-phase five-level H- bridge inverter	82
3.4	Mapping voltage vector of five-level CHB	83
3.5	The selected vector of five-level CHB mapping voltage vector	84
3.6	The workflow of voltage vectors for sector aligned to q-axis based on: (a) circular stator flux locus, and (b) hexagonal diagram	85
3.7	The workflow of voltage vectors for sector aligned to d-axis based on: (a) circular stator flux locus, and (b) hexagonal diagram	85
3.8	Stator flux vector control for tracking its reference with a suitable voltage vector application	93
3.9	The phasor diagram of stator voltage, ohmic voltage drop and back-emf	95

	vector at: (a) low and (b) high operating speed	
3.10	The selection of voltage to control the operation of torque and flux in the conventional (solid line) and proposed (dotted line) DTC method at low_1 operating speed	98
3.11	The selection of voltage to control the operation of torque and flux in the conventional (solid line) and proposed (dotted line) DTC method at low_2 operating speed	100
3.12	The selection of voltage to control the operation of torque and flux in the conventional (solid line) and proposed (dotted line) DTC method at medium_1 operating speed	101
3.13	The selection of voltage to control the operation of torque and flux in the conventional (solid line) and proposed (dotted line) DTC method at medium_2 operating speed	102
3.14	The selection of voltage to control the operation of torque and flux in the conventional (solid line) and proposed (dotted line) DTC method at high_1 operating speed	104
3.15	The selection of voltage to control the operation of torque and flux in the conventional (solid line) and proposed (dotted line) DTC method at high_2 operating speed	105
3.16	The torque variation in the hysteresis band to control the operation of torque in the conventional (solid line) and proposed (dotted line) DTC method at low_1 operating speed	107
3.17	The torque variation in the hysteresis band to control the operation of torque in the conventional (solid line) and proposed (dotted line) DTC method at low_2 operating speed	108

3.18	The torque variation in the hysteresis band to control the operation of torque in the conventional (solid line) and proposed (dotted line) DTC method at medium_1 operating speed	109
3.19	The torque variation in the hysteresis band to control the operation of torque in the conventional (solid line) and proposed (dotted line) DTC method at medium_2 operating speed	110
3.20	The torque variation in the hysteresis band to control the operation of torque in the conventional (solid line) and proposed (dotted line) DTC method at high_1 operating speed	111
3.21	The torque variation in the hysteresis band to control the operation of torque in the conventional (solid line) and proposed (dotted line) DTC method at high_2 operating speed	112
3.22	The proposed structure of DTC fed by five-level CHB by using optimal switching strategy	117
3.23	The DTC structure by using fixed sector rotation strategy (W.S.H and Holliday, 2004)	118
3.24	The shifted sector by using fixed sector rotation strategy (W.S.H and Holliday, 2004)	119
3.25	The graph of speed against shifted angle and flux droop at torque of 1.5 Nm	120
3.26	The graph of speed against shifted angle at the various reference torque	122
3.27	The graph of speed interception against reference torque	124
3.28	The proposed structure of DTC by using optimal sector rotation strategy	125
3.29	MATLAB/Simulink simulation model of conventional DTC	127

3.30	MATLAB/Simulink simulation model of proposed optimal DTC switching strategy	127
3.31	MATLAB/Simulink simulation model of proposed optimal sector rotation strategy	128
3.32	MATLAB/Simulink simulation model of flux comparator	129
3.33	MATLAB/Simulink simulation model of torque controller	129
3.34	MATLAB/Simulink simulation model of three-phase induction motor	130
3.35	MATLAB/Simulink simulation model of stator voltage d- and q- component for two-level inverter	131
3.36	MATLAB/Simulink simulation model of stator voltage d- and q- component for five-level inverter	131
3.37	MATLAB/Simulink simulation model of the estimation of electromagnetic torque and stator flux	132
3.38	MATLAB/Simulink simulation model of new modification torque error status	133
3.39	MATLAB/Simulink simulation model of new modification of sector detection	134
3.40	The flowchart of detection of flux sector	135
3.41	The layout diagram of the entire setup of DTC drive system	137
3.42	The experimental setup of DTC drive system	137
3.43	The dSPACE 1104 Controller Board	138
3.44	Layout design of current measurement circuit	140
3.45	Hardware prototype of current measurement circuit	141
3.46	Hardware prototype of FPGA board with level shifter circuit	142
3.47	The generation of blanking time by using FPGA	143

3.48	The block diagram of signal generation process of FPGA	144
3.49	Layout design of gate driver circuit	145
3.50	Layout design of three-phase five-level CHB inverter circuit	146
3.51	Hardware prototype design of single-phase H-bridge inverter with gate driver circuit	147
3.52	Hardware prototype of three-phase five-level CHB inverter circuit	147
3.53	The setup of three-phase induction machine with DC generator as a loading unit	148
4.1	The comparison of switching frequency at low_1 operating speed between; (a) the conventional method and (b) the proposed method	153
4.2	The comparison of switching frequency at low_2 operating speed between; (a) the conventional method and (b) the proposed method	154
4.3	The comparison of switching frequency at medium_1 operating speed between; (a) the conventional method and (b) the proposed method	155
4.4	The comparison of switching frequency at medium_2 operating speed between; (a) the conventional method and (b) the proposed method	156
4.5	The comparison of switching frequency at high_1 operating speed between; (a) the conventional method and (b) the proposed method	157
4.6	The comparison of switching frequency at high_2 operating speed between; (a) the conventional method and (b) the proposed method	158
4.7	The experimental results of torque, T_e (upper), phase current, I_s (middle) and phase voltage, V_s (lower) in; (a) real picture and (b) magnified picture at low_1 operating speed	162
4.8	The simulation results of torque, T_e (upper), phase current, I_s (middle) and phase voltage, V_s (lower) in; (a) real picture and (b) magnified	162

	picture at low_1 operating speed	
4.9	The experimental results of torque, T_e (upper), phase current, I_s (middle) and phase voltage, V_s (lower) in; (a) real picture and (b) magnified picture at low_2 operating speed	163
4.10	The simulation results of torque, T_e (upper), phase current, I_s (middle) and phase voltage, V_s (lower) in; (a) real picture and (b) magnified picture at low_2 operating speed	164
4.11	The experimental results of torque, T_e (upper), phase current, I_s (middle) and phase voltage, V_s (lower) in; (a) real picture and (b) magnified picture at medium_1 operating speed	165
4.12	The simulation results of torque, T_e (upper), phase current, I_s (middle) and phase voltage, V_s (lower) in; (a) real picture and (b) magnified picture at medium_1 operating speed	165
4.13	The experimental results of torque, T_e (upper), phase current, I_s (middle) and phase voltage, V_s (lower) in; (a) real picture and (b) magnified picture at medium_2 operating speed	166
4.14	The simulation results of torque, T_e (upper), phase current, I_s (middle) and phase voltage, V_s (lower) in; (a) real picture and (b) magnified picture at medium_2 operating speed	167
4.15	The experimental results of torque, T_e (upper), phase current, I_s (middle) and phase voltage, V_s (lower) in; (a) real picture and (b) magnified picture at high_1 operating speed	168
4.16	The simulation results of torque, T_e (upper), phase current, I_s (middle) and phase voltage, V_s (lower) in; (a) real picture and (b) magnified picture at high_1 operating speed	168

4.17	The experimental results of torque, T_e (upper), phase current, I_s (middle) and phase voltage, V_s (lower) in; (a) real picture and (b) magnified picture at high_2 operating speed	169
4.18	The simulation results of torque, T_e (upper), phase current, I_s (middle) and phase voltage, V_s (lower) in; (a) real picture and (b) magnified picture at high_2 operating speed	170
4.19	Stator flux (upper), φ_s sector, θ_n and modified sector, θ_n' (lower) through the; (a) experimental and (b) simulation result at 500 rpm	173
4.20	Stator flux (upper), φ_s sector, θ_n and modified sector, θ_n' (lower) through the; (a) experimental and (b) simulation result at 450 rpm	174
4.21	Stator flux (upper), φ_s sector, θ_n and modified sector, θ_n' (lower) through the; (a) experimental and (b) simulation result at 300 rpm	174
4.22	Stator flux (upper), φ_s sector, θ_n and modified sector, θ_n' (lower) through the; (a) experimental and (b) simulation result at 200 rpm	175
4.23	Stator flux (upper), φ_s sector, θ_n and modified sector, θ_n' (lower) through the; (a) experimental and (b) simulation result at 150 rpm	175
4.24	(a) The experimental and (b) simulation result of stator flux, φ_s (upper), sector, θ_n and modified sector, θ_n' (lower) for the torque of 1.9 Nm at 450 rpm	177
4.25	(a) The experimental and (b) simulation result of stator flux, φ_s (upper), sector, θ_n and modified sector, θ_n' (lower) for the torque of 1.5 Nm at 450 rpm	177
4.26	(a) The experimental and (b) simulation result of stator flux, φ_s (upper), sector, θ_n and modified sector, θ_n' (lower) for the torque of 1.1 Nm at 450 rpm	178

4.27	(a) The experimental and (b) simulation result of stator flux, φ_s (upper), sector, θ_n and modified sector, θ_n' (lower) for the torque of 1.9 Nm at 300 rpm	178
4.28	(a) The experimental and (b) simulation result of stator flux, φ_s (upper), sector, θ_n and modified sector, θ_n' (lower) for the torque of 1.5 Nm at 300 rpm	179
4.29	(a) The experimental and (b) simulation result of stator flux, φ_s (upper), sector, θ_n and modified sector, θ_n' (lower) for the torque of 1.1 Nm at 300 rpm	179
4.30	(a) The experimental and (b) simulation result of stator flux, φ_s (upper), sector, θ_n and modified sector, θ_n' (lower) for the torque of 1.9 Nm at 200 rpm	180
4.31	(a) The experimental and (b) simulation result of stator flux, φ_s (upper), sector, θ_n and modified sector, θ_n' (lower) for the torque of 1.5 Nm at 200 rpm	180
4.32	(a) The experimental and (b) simulation result of stator flux, φ_s (upper), sector, θ_n and modified sector, θ_n' (lower) for the torque of 1.1 Nm at 200 rpm	180
4.33	The experimental results of torque, T_e (upper), phase voltage, V_s (middle) and speed, ω_m (lower) for the torque at; (a)1 Nm and (b)1.5 Nm at steady-state operation	182
4.34	The simulation results of torque, T_e (upper), phase voltage, V_s (middle) and speed, ω_m (lower) for the torque at; (a)1 Nm and (b)1.5 Nm at steady-state operation	183
4.35	The experimental results of stator flux, φ_s (upper) and phase current, I_s	184

	(lower) for the torque at; (a)1 Nm and (b)1.5 Nm at steady-state operation	
4.36	The simulation results of stator flux, φ_s (upper) and phase current, I_s (lower) for the torque at; (a)1 Nm and (b)1.5 Nm at steady-state operation	184
4.37	The experimental results of torque, T_e (upper), phase voltage, V_s (middle) and speed, ω_m (lower) in the conventional method for the conversion of torque from; (a)1.5 Nm to 1 Nm, and (b)1 Nm to 1.5 Nm	185
4.38	The simulation results of torque, T_e (upper), phase voltage, V_s (middle) and speed, ω_m (lower) in the conventional method for the conversion of torque from; (a)1.5 Nm to 1 Nm, and (b)1 Nm to 1.5 Nm	185
4.39	The experimental results of stator flux, φ_s (upper) and phase current, I_s (lower) in the conventional method for the conversion of torque from; (a)1.5 Nm to 1 Nm, and (b)1 Nm to 1.5 Nm	186
4.40	The simulation results of stator flux, φ_s (upper) and phase current, I_s (lower) in the conventional method for the conversion of torque from; (a)1.5 Nm to 1 Nm, and (b)1 Nm to 1.5 Nm	187
4.41	The experimental results of torque, T_e (upper), modified angle, $\Delta\theta'$ (middle) and speed, ω_m (lower) in the proposed method for the conversion of torque from; (a)1.5 Nm to 1 Nm, and (b)1 Nm to 1.5 Nm.	188
4.42	The simulation results of torque, T_e (upper), modified angle, $\Delta\theta'$ (middle) and speed, ω_m (lower) in the proposed method for the conversion of torque from; (a)1.5 Nm to 1 Nm, and (b)1 Nm to 1.5 Nm	188
4.43	The experimental results of stator flux, φ_s (upper) and phase current, I_s (lower) in the proposed method for the conversion of torque from;	189